

# Roughness of Brittle Fractures as a Correlated Percolation Problem

Jan Øystein H. Bakke<sup>1</sup>, Johannes Bjelland<sup>1</sup>, Thomas Ramstad<sup>1</sup>, Torunn Strandén<sup>1</sup>, Alex Hansen<sup>1</sup> and Jean Schmittbuhl<sup>2</sup>

<sup>1</sup>Department of Physics, Norwegian University of Science and Technology, N-7491 Trondheim, Norway

<sup>2</sup>Laboratoire de Géologie, UMR CNRS 8538, Ecole Normale Supérieure, 24, rue Lhomond, F-75231 Paris Cédex 05, France

Received March 22, 2003; accepted April 8, 2003

PACS Ref: 83.80.Ab, 62.20.Mk, 81.40.Np

This paper is dedicated to Professor Dietrich Stauffer on the occasion of his sixtieth birthday.

## Abstract

The morphology of brittle fracture surfaces are self affine with roughness exponents that may be classified into a small number of universality classes. We discuss these in light of the recent proposal that the self affinity is a manifestation of the fracture process being a correlated percolation process. We also study numerically with high precision the roughness exponent in the two-dimensional fuse model with disorder both in breaking thresholds and conductances of the fuses. Our results are consistent with the predictions of the correlated percolation theory.

The fracture of brittle materials is a phenomenon that has received much attention throughout history for obvious practical reasons: In order for us to be able to rely on our human-made constructions, we need to understand why they fail and how they fail. However, it is only during the past fifteen or so years that this subject has interested the statistical physics community [1]. It is still regarded somewhat as “unconventional” by, at least, parts of the statistical physics community. However, over the last few years, the approach to brittle fracture that has emerged from this community has spurred the interest of those communities traditionally working on fracture phenomena.

It is in particular the similarities between the fracture process and dynamical critical phenomena that has triggered the imagination of workers in statistical physics, see, e.g. Refs. [2–4]. The aspect of the brittle fracture phenomenon that has received most attention in this context, is the morphology of fracture surfaces. It turns out that such surfaces show surprising scaling properties [5]. These were first seen in the mid eighties [6,7]. They manifest themselves through self-affine long-range height correlations. That is, the conditional probability density  $\pi(x, y)$ , i.e. the probability that the crack surface passes within dy of the height y at position x when it had height zero at  $x = 0$ , shows the invariance

$$\lambda^\zeta \pi(\lambda x, \lambda^\zeta y) = \pi(x, y), \quad (1)$$

where  $\zeta$  is the roughness exponent. In the early nineties increasing experimental evidence hinted at the roughness exponent not only existed, but had a *universal* value of about 0.80 [8–12].

It turns out, however, that this picture is not the whole story: At small scales, there is a *second* universal regime with a roughness exponent of about 0.5 [13,14]. There is a clear crossover length scale between the small and large scale scaling regimes. Curiously, the same small-scale roughness exponent,  $\zeta = 0.5$ , is also found on large scales for sandstone where the fracture process is strongly intergranular [15,16].

Fracture morphology has also been studied for two-dimensional brittle systems. Using paper [17], a roughness exponent in the range  $\zeta = 0.63$  to 0.72 was found, while experiments on thin wood plates cut orthogonally to the grain direction, gave  $\zeta = 0.68 \pm 0.04$  [18]. No small-scale regime has so far been identified for two-dimensional systems.

Much work has been invested in understanding why fracture surfaces are self affine and why their roughness seems to fall into a small number of distinct universality classes, see [19–34]. Much of this work has been focused on the quasi-static fuse model [1] as a paradigm for brittle fracture. The quasi-static fuse model consists of a lattice where each bond is an ohmic resistor as long as the electrical current it carries is below a threshold value. If the threshold is passed, the bond burns out irreversibly. The threshold  $t$  of each bond is drawn from an uncorrelated distribution  $\tilde{p}(t)$ , while the bonds all have the same conductance. The lattice is placed between electrical bus bars and an increasing current is passed through it. Numerically, the Kirchhoff equations are solved with a voltage difference between the bus bars set to unity. The ratio between current  $i_j$  and threshold  $t_j$  for each bond  $j$  is calculated and the bond having the largest value,  $\max_j (i_j/t_j)$  is identified and subsequently irreversibly removed.

In the limit of infinite disorder—i.e., when the threshold distribution is on the verge of becoming non-normalizable, e.g.  $\tilde{p}(t) \propto t^{-\alpha-1}$ , where  $1 \leq t < \infty$  in the limit of  $\alpha \rightarrow 0$ , the fuse problem becomes equivalent to a bond percolation problem [35]. At more narrow disorders, a rich phase diagram appears which is controlled by two parameters, the exponent  $\alpha$  which controls the threshold distribution tail toward infinitely large threshold values and the exponent  $\beta$  which controls the tail of the threshold distribution toward zero:  $\tilde{p}(t) \propto t^{-1+\beta}$  where  $0 \leq t \leq 1$  [36]. For smaller values of either  $\alpha$  or  $\beta$ , the fuse model still shows behavior very similar to percolation: The lattice stops conducting after a finite percentage of bonds have burned out even when the lattice size is extrapolated to infinity. Close to breakdown, critical

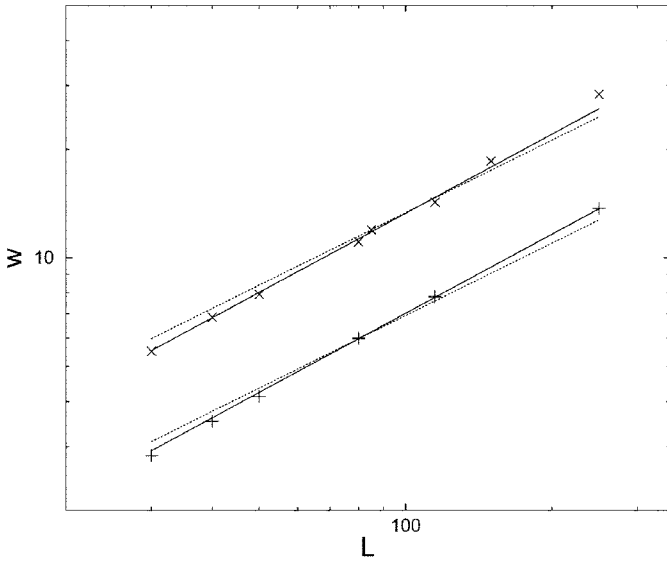


Fig. 1. Fracture width  $w$  as a function of system size  $L_x = L_y = L$  for threshold distributions  $\tilde{p}(t) \propto t^{-\alpha-1}$  with  $\alpha = 2$  for  $1 \leq t < \infty$  (+) and  $\tilde{p}(t) \propto t^{\beta-1}$  with  $\beta = 2$  for  $0 \leq t \leq 1$  (x). The second data set has been scaled by a factor two to separate it from the first set. The straight unbroken lines are  $w \sim L^{8/11}$ . The straight broken lines are  $w \sim L^{2/3}$ .

exponents may be defined precisely as in the percolation problem. However, as the breakdown process in the fuse model is highly correlated, there is no *a priori* reason to expect these exponents to be equal to those found in the percolation problem. At even smaller disorders, localization sets in.

When the disorder is broad enough so that the fuse model behaves in a percolation-like manner—i.e., there is no localization of the fracture process as it proceeds—there is a diverging correlation length  $\xi \propto |p - p_c|^{-\nu}$ , where  $p$  is the density of broken bonds and  $p_c$  is the density at which an infinite lattice breaks down. For classical percolation,  $\nu = 4/3$  [37]. In Ref. [34],  $\nu$  was measured for different sufficiently broad but finite disorders, finding a value indistinguishable from the percolation value,  $4/3$ . Hence, it

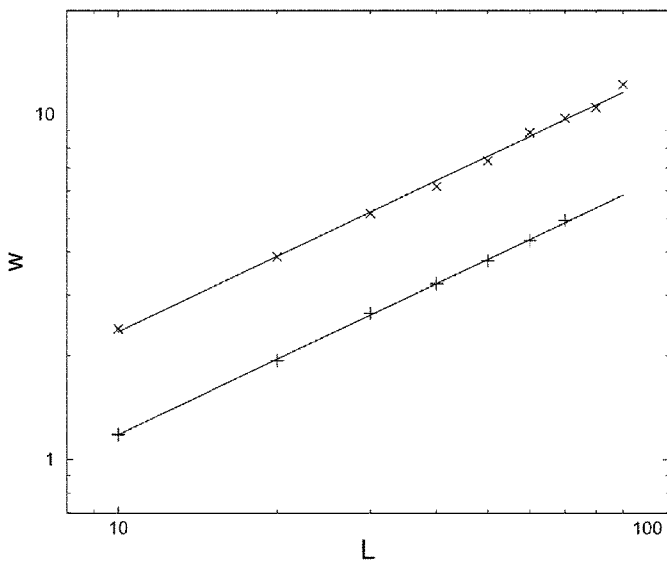


Fig. 2. Fracture width  $w$  as a function of system size  $L_x = L_y = L$  for conductance distributions  $\tilde{p}(g) \propto (g - g_0)^{\beta-1}$  on the interval  $g_0 \leq g \leq 1 + g_0$ , where we have chosen  $\beta = 1/2$  and  $g_0 = 0.001$  (+) and  $g_0 = 0.01$  (x). The second data set has been scaled by a factor two to separate it from the first set. The straight lines are  $w \sim L^{8/11}$ .

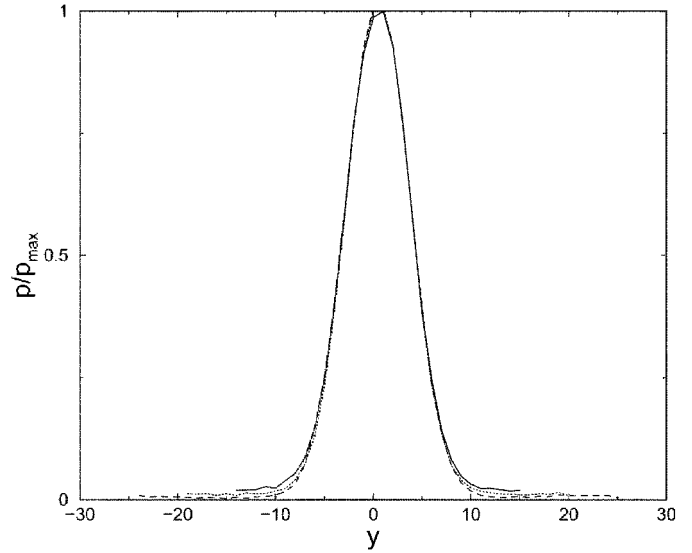


Fig. 3. Damage profile for fixed width  $L_x = 30$  and lengths  $L_y = 30, 40$  and  $50$  for the fuse model with breaking thresholds distributed according to  $\tilde{p}(t) \propto t^{-\alpha-1}$  in the range  $1 \leq t < \infty$ , with  $\alpha = 2$ .

was concluded that the two-dimensional fuse model is in the percolation universality class when the disorder is broad enough to produce a non-localized fracture. A recent study [40] gives  $\nu = 0.86 \pm 0.06$  for the three-dimensional fuse model. This is indistinguishable from the three-dimensional percolation problem, where  $\nu = 0.88$ . Hence, we draw the same conclusion in this case: The fuse model is in the universality class of percolation for disorder broad enough not to produce localization.

At smaller disorders so that there is localization, the fuse model produces self-affine fracture lines in two dimensions [19] and surfaces in three dimensions [26,27]. A consequence of the scaling properties of the conditional probability  $\pi$ , Eq. (1), is that the width of the fracture line,  $w = \sqrt{\langle y^2 \rangle - \langle y \rangle^2}$ , scales as

$$w \sim L_x^\xi, \tag{2}$$

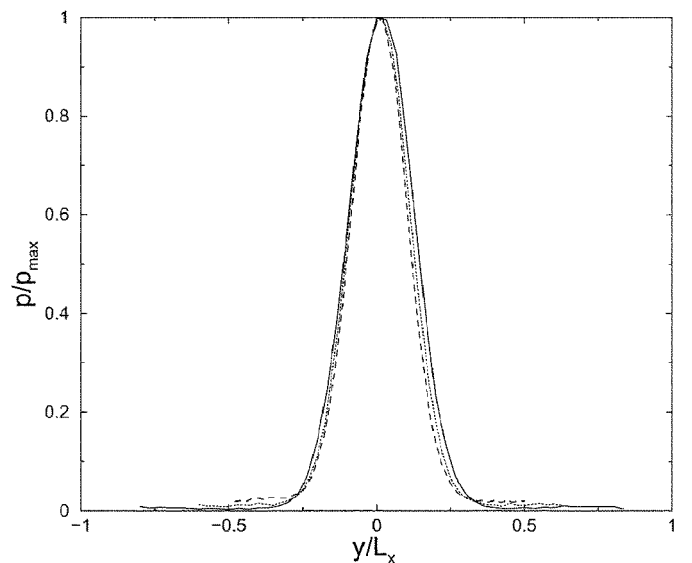


Fig. 4. Damage profile for fixed length  $L_y = 50$  and widths  $L_x = 30, 40$  and  $50$  for the fuse model with breaking thresholds distributed according to  $p(t) \propto t^{-\alpha-1}$  in the range  $1 \leq t < \infty$ , with  $\alpha = 2$ .

where  $L_x$  is the width of the lattice in the  $x$  direction. In Fig. 1, we show fracture width as a function of system width,  $L_x$  for square lattices, so that  $L_y = L_x = L$ . In order to minimize corrections due to finite size effects, we have implemented biperiodic boundary conditions (periodicity in all directions) [41]. However, in order to avoid spiralling fracture lines, one row of fuses in the direction orthogonal to the average current direction was made unbreakable. The square lattice was oriented at  $45^\circ$  with respect to the average current direction so that before any bonds have broken, they all carry the same current. In Ref. [19], it was suggested that the roughness of the fracture lines in the two-dimensional fuse model might be in the universality class of the directed polymer problem [38,39]. If this were true, the roughness exponent would be  $\zeta = 2/3$ . We show in Fig. 1,  $w \sim L_x^{2/3}$  (broken lines). Clearly,  $\zeta = 2/3$  is *not* consistent with our data. This is the opposite conclusion from that presented in Refs [27,29]. Our estimate of the roughness exponent from our data is  $\zeta = 0.74 \pm 0.02$ . In Fig. 2, we keep the thresholds constant equal to one, while the conductances of the bonds are distributed according to  $\tilde{p}(g) \propto (g - g_0)^{\beta-1}$  on the interval  $g_0 \leq g \leq 1 + g_0$ . We find a roughness exponent  $\zeta = 0.74 \pm 0.03$ . Hence, disorder in the thresholds or in the conductances lead to the same fracture morphology.

In Ref. [34], it was proposed that the roughness exponent is a manifestation of the same critical behavior that is seen when the disorder in the system is large enough that the fracture process proceeds without localization. The key idea is based on the classic study of the percolation problem in a constant control parameter gradient [42]. When the fracture process localizes, a damage profile,  $p(y)$ , as shown in Fig. 3 develops. It has a quadratic maximum and width  $l$ . This width is independent of the length of the system,  $L_y$  as shown in the figure. On the other hand, the localization length is proportional to the width of the lattice,  $L_x$ ,

$$l \propto L_x. \quad (3)$$

This is shown in Fig. 4, where we show data collapse using the reduced variable  $y/L_x$ . A qualitative argument for this is [34] to note that each broken bond creates a disturbance in the average current field that enhances the probability for a new bond to break in a finite-width cone which stretches out from each side of the bond in the direction approximately orthogonal to the average current direction. Hence, as long as the current enhancement is not sufficient to induce crack coalescence and create an unstable crack tip, the damage zone will spread in the new cones in a random fashion. This argument has been made quantitative in a mean field context [43].

The maximum of the damage profile,  $p(y)$ , occurs at  $y = y_c$ . Around this maximum it behaves as

$$p(y) - p(y_c) \propto \left(\frac{y - y_c}{l}\right)^2. \quad (4)$$

When the system is broken apart, the fatal fracture line (i.e. the one breaking the network in two) will be centered at the position of the maximum of the damage profile,  $y_c$ . Around this maximum, there will be a critical region, where the

fracture process has proceeded in the same way as when the disorder is wide enough so that localization does not occur. This must be so since, this region is much more narrow than the localization length,  $l$ . Within this region, the system will be close to a critical state at failure. However, the correlation length,  $\xi$ , cannot be infinite since the damage falls off on both sides of  $y_c$ . Hence, the shape of the damage profile determines the size of  $\xi$ . Using Eq. (4), we may define  $y_{\pm} = y_c \pm \xi$ , so that

$$p(y_{\pm}) - p(y_c) \propto \left(\frac{y_{\pm} - y_c}{l}\right)^2 \propto \left(\frac{\xi}{l}\right)^2. \quad (5)$$

If we now use the relation between correlation length and control parameter,

$$\xi \sim |p(y_c) - p(y_{\pm})|^{-\nu}, \quad (6)$$

we may eliminate  $[p(y_c) - p(y_{\pm})]$  between this equation and Eq. (5) to get

$$\xi \sim l^{2\nu/(1+2\nu)}. \quad (7)$$

The fracture line will not be localized in the critical region of width  $\xi$ . In the same way it is not localized when the disorder is wide enough so that the entire fracture process is not localized. Hence, we must have that

$$w \propto \xi. \quad (8)$$

We now combine Eqs. (3), (7) and (8) to get

$$w \sim L_x^{2\nu/(1+2\nu)}. \quad (9)$$

Comparing this equation with Eq. (2), we conclude that

$$\zeta = \frac{2\nu}{1+2\nu}. \quad (10)$$

Hence, if the correlation length exponent is  $\nu = 4/3$  in two dimensions, the roughness exponent becomes  $\zeta = 8/11 \approx 0.73$ , while with  $\nu = 0.88$  in three dimensions, we find  $\zeta = 0.64$ . This prediction [34] is compared to our two-dimensional data in Figs. 1 and 2, while the three-dimensional prediction should be compared to the numerical measurement of Ref. [26] giving  $\zeta = 0.62 \pm 0.05$ . We note, however, that the three-dimensional prediction is not consistent with [27], who found a roughness exponent close to the minimal energy result,  $\zeta = 0.41 \pm 0.02$  [44]. This is the three-dimensional equivalent of the directed polymer problem in two dimensions giving  $\zeta = 2/3$  in this case.

We show in the last column of Table I the roughness exponents measured for different systems. In addition to the fuse model, there are two other network models that are of particular interest: The beam model and the central force model [1]. The beam model consists of a network of elastic beams that are rigidly connected at the nodes. On lattices with higher symmetry than the square one, this system is describable by the Cosserat generalized elastic equations [1,45]. Cosserat elasticity includes rotational degrees of freedom in addition to the translational ones on the strain field. This is in contrast to the usual elastic Lamé equations, which only include translational degrees of freedom. The Cosserat equations are used to describe

Table I. Correlation exponents, roughness exponents calculated from these using Eq. (10), and measured roughness exponents. The question marks signify that the exponents have not yet been calculated or measured numerically or experimentally.

Model	$\nu$	$2\nu/(1+2\nu)$	$\zeta$
2D fuse	4/3	8/11	$0.74 \pm 0.02$
3D fuse	0.88	0.64	$0.62 \pm 0.05$
2D beam	2.83 <sup>a</sup>	0.85	$0.86 \pm 0.03$
3D beam	?	?	?
2D centr. force	$1.16 \pm 0.03$	0.70	?
3D centr. force	?	?	?
2D br. frac. <sup>b</sup>	?	?	?
2D br. frac.	?	?	$0.68 \pm 0.04$
3D br. frac. <sup>c</sup>	?	?	0.5
3D br. frac.	2	4/5	0.80

<sup>a</sup>This exponent has been measured numerically for a network of freely rotating bendable beams.  $\nu$  is here the correlation exponent that characterizes the phase in which bending forces dominate [48].

<sup>b</sup>Small scale.

<sup>c</sup>Small scale.

granular materials, such as porous media or crystallite materials. There is always a length scale associated with the granularity, and such materials are described by the Lamé equations on scales larger than this length scale. The central force network consists of Hookean springs that rotate freely about the nodes. In the continuum limit, this model is described by the Lamé elastic equations.

As seen in Table I, only the roughness exponent for the beam model in two-dimensions (on a square lattice) has been measured [30]. Numerical calculations of the roughness exponent for the two-dimensional central force are, however, underway [46]. The correlation length exponent has been measured for the central-force network [47] to be  $1.16 \pm 0.03$ . No direct measurement of this quantity has been performed for the beam network. However, in a somewhat similar model, the “Mikado” model, where slender beams are placed at random, and where they overlap, they are hinged and can rotate freely about these. In Ref. [48], a correlation length has been identified with the transition from bending forces dominating the network to compressional forces dominating. The corresponding correlation length exponent was measured to be 2.83. If we now use Eq. (10) to calculate the corresponding roughness exponents, we find  $\zeta = 0.70$  for the central-force model in two dimensions and  $\zeta = 0.85$  for the two-dimensional beam model (see Table I). The second value, corresponding to the square beam lattice, matches the numerical value of Ref. [30],  $\zeta = 0.86 \pm 0.03$ , very well.

Three roughness exponents are known for brittle fracture in two and three dimensions:  $\zeta = 0.68 \pm 0.04$  in two dimensions and 0.5 on small scales and 0.80 on large scales in three dimensions. There exists an analytical calculation of  $\nu$  for three-dimensional brittle fracture going beyond mean field theory [33]. The result is  $\nu = 2$ . Eq. (10) leads to  $\zeta = 4/5$ , which matches the experimentally observed large scale value perfectly.

It has recently been proposed that the small scale roughness exponent seen in three-dimensional brittle fracture,  $\zeta = 0.5$ , is caused by elastic corrugation waves [32]. However, it is difficult to reconcile this theory with the

observed 0.5-exponent in sandstone. Either the roughness exponent seen at small scales is unrelated to the large scale exponent seen in sandstone—in which case there is no problem, or the two exponents are caused by the same mechanism—in which case it becomes difficult to accept the corrugation wave theory. Here, we follow [49] and propose an alternative explanation for the existence of different roughness exponents at small ( $\zeta = 0.5$ ) and large scales ( $\zeta = 0.80$ ) in the same material.

Sandstone and crystallite materials are described by Cosserat elasticity on small scale and Lamé elasticity on large scale. The roughness measurements on sandstone that have been reported [15,16] are in fact small-scale measurements with respect to grain sizes of such materials. As the critical behavior of the beam and central force lattices are different, we find different fracture roughness for the two types of elasticity. Hence, we propose that the small-scale exponent seen in three-dimensional brittle fracture in fact is a “Cosserat” roughness exponent, while the roughness exponent seen on large scale is a “Lamé” roughness exponent. We note from Table I that the prediction for the central-force network is  $\zeta = 0.70$  in two dimensions. This matches very well the value seen experimentally in two-dimensional brittle fracture,  $\zeta = 0.68 \pm 0.04$ . This value is based on Lamé elasticity, and is thus a large-scale exponent. We expect there to be a small-scale two-dimensional roughness exponent that corresponds to Cosserat elasticity, equal to 0.86. The large scale three-dimensional exponent equal to 0.80 is a “Lamé” exponent, and we expect that this value will be found for the three-dimensional central-force network. The small scale three-dimensional roughness exponent should be found in a three-dimensional beam lattice.

Even though brittle fracture is no longer a newcomer in statistical physics, the field is by no means in any way slowing down. Rather, the opposite is true. The recent surge in interest in the statistical physics approach from the more traditional communities working in this field is generating a cross fertilization that promises to supply us with interesting problems for a long time to come.

## Acknowledgements

We thank B. Chakrabarti for the opportunity to present this work in the friendly setting of "Conference on Unconventional Applications of Statistical Physics" at the Saha Institute for Nuclear Physics in Kolkata. A.H. thanks Dietrich Stauffer for the countless advice on computational physics, physics and everything else through the last fifteen years and congratulates him on the occasion of his sixtieth birthday.

## References

1. Herrmann, H. J. and Roux, S., (Eds.) "Statistical Models for the Fracture of Disordered Media" (North-Holland, Amsterdam, 1990).
2. Hansen, A. and Hemmer, P. C., *Trends Statistical Phys.* **1**, 213 (1994).
3. Sornette, D., "Critical Phenomena in Natural Sciences," (Springer Verlag, Berlin, 2000).
4. Pradhan, S., Bhattacharyya, P. and Chakrabarti, B., *Phys. Rev. E* **67**, 016116 (2002).
5. Bouchaud, E., *J. Phys. Condens. Matt.* **9**, 4319 (1997).
6. Mandelbrot, B. B., Passoja, D. E. and Paullay, A. J., *Nature* **308**, 721 (1984).
7. Brown, S. R. and Scholz, C. H., *J. Geophys. Res.* **90**, 12575 (1985).
8. Bouchaud, E., Lapasset, G. and Planès, J., *Europhys. Lett.* **13**, 73 (1990).
9. Måløy, K. J., Hansen, A., Hinrichsen, E. L. and Roux, S., *Phys. Rev. Lett.* **68**, 213 (1992).
10. Schmittbuhl, J., Gentier, S. and Roux, S., *Geophys. Res. Lett.* **20**, 639 (1993).
11. Cox, B. L. and Wang, J. S. Y., *Fractals* **1**, 87 (1993).
12. Schmittbuhl, J., Schmitt, F. and Scholz, C. H., *J. Geophys. Res.* **100**, 5953 (1995).
13. Daguier, P., Henaux, S., Bouchaud, E. and Creuzet, F., *Phys. Rev. E* **53**, 5637 (1996).
14. Daguier, P., Nghiem, B., Bouchaud, E. and Creuzet, F., *Phys. Rev. Lett.* **78**, 1062 (1997).
15. Boffa, J. M., Allain, C. and Hulin, J. P., *Eur. Phys. J. App. Phys.* **2**, 281 (1998).
16. Méheust, Y., Ph.D. Thesis, Université Paris XI (2002).
17. Kertész, J., Horváth, V. and Weber, F., *Fractals* **1**, 67 (1993).
18. Engoy, T., Måløy, K. J., Hansen, A. and Roux, S., *Phys. Rev. Lett.* **73**, 834 (1994).
19. Hansen, A., Hinrichsen, E. L. and Roux, S., *Phys. Rev. Lett.* **66**, 2476 (1991).
20. Bouchaud, J. P., Bouchaud, E., Lapasset, G. and Planès, J., *Phys. Rev. Lett.* **71**, 2240 (1993).
21. Mosolov, A. B., *Europhys. Lett.* **24**, 673 (1993).
22. Bouchaud, E. and Bouchaud, J. P., *Phys. Rev. B* **50**, 17752 (1994).
23. Ramanathan, S., Ertas, D. and Fisher, D. S., *Phys. Rev. Lett.* **79**, 873 (1997).
24. Omeltchenko, A., Yu, J., Kalia, R. K. and Vashishta, P., *Phys. Rev. Lett.* **78**, 2148 (1997).
25. Räsänen, V. I., Alava, M. J. and Nieminen, R. M., *Phys. Rev. B* **58**, 14288 (1998).
26. Batrouni, G. G. and Hansen, A., *Phys. Rev. Lett.* **80**, 325 (1998).
27. Räsänen, V. I., Seppälä, E. T., Alava, M. J. and Duxbury, P. M., *Phys. Rev. Lett.* **80**, 329 (1998).
28. Lung, C. W., Jiang, J., Tian, E. K. and Zhang, C. H., *Phys. Rev. E* **60**, 5121 (1999).
29. Seppälä, E. T., Räsänen, V. I. and Alava, M. J., *Phys. Rev. E* **61**, 6312 (2000).
30. Skjetne, B., Helle, T. and Hansen, A., *Phys. Rev. Lett.* **87**, 125503 (2001).
31. Barra, F., Hentchel, H. G., Levermann, A. and Procaccia, I., *Phys. Rev. E* **65**, 045101 (2002).
32. Bouchaud, E., Bouchaud, J. P., Fisher, D. S., Ramanathan, S. and Rice, J. R., *J. Mech. Phys. Solids* **50**, 1703 (2002).
33. Toussaint, R. and Pride, S. R., *Phys. Rev. E* **66**, 036135 (2002); *Phys. Rev. E*, **66**, 036136 (2002); *Phys. Rev. E*, **66**, 036137 (2002).
34. Hansen, A. and Schmittbuhl, J., *Phys. Rev. Lett.* **90**, 045504 (2003).
35. Roux, S., Hansen, A., Herrmann, H. J. and Guyon, E., *J. Stat. Phys.* **52**, 237 (1988).
36. Hansen, A., Hinrichsen, E. L. and Roux, S., *Phys. Rev. B* **43**, 665 (1991).
37. Stauffer, D. and Aharony, A., "Introduction to Percolation Theory," (Taylor and Francis, London, 1992).
38. Barabási, A.-L. and Stanley, H. E. "Fractal Concepts in Surface Growth," (Cambridge UP, 1995).
39. Halpin-Healy, T. and Zhang, Y.-C., *Phys. Rep.* **254**, 215 (1995).
40. Ramstad, T., Bakke, J. Ø. H., Bjelland, J., Stranden, T. and Hansen, A., in preparation (2003).
41. Roux, S., unpublished.
42. Sapoval, B., Rosso, M. and Gouyet, J.F., *J. Phys. Lett. (France)* **46**, L149 (1985).
43. Toussaint, R. and Hansen, A., in preparation (2003).
44. Alava, M. J. and Duxbury, P. M., *Phys. Rev. Lett.* **54**, 14990 (1996).
45. Love, A. E. H., "A Treatise on the Mathematical Theory of Elasticity," (Dover, New York, 1944).
46. Bakke, J. Ø. H. and Hansen, A., in preparation (2003).
47. Moukarzel, C. and Duxbury, P. M., *Phys. Rev. E* **59**, 2614 (1999).
48. Wilhelm, J. and Frey, E., *Cond-mat/0303592* (2003).
49. Hansen, A. and Schmittbuhl, J., in preparation (2003).